

# Roughness reduction of large-area high-quality thick Al films for echelle gratings by multi-step deposition method

Zizheng Li,<sup>1,2</sup> Jinsong Gao,<sup>1</sup> Haigui Yang,<sup>1,\*</sup> Tongtong Wang,<sup>1</sup> and Xiaoyi Wang<sup>1</sup>

<sup>1</sup>Key Laboratory of Optical System Advanced Manufacturing Technology, Changchun Institute of Optics, Fine Mechanics and Physics, Chinese Academy of Sciences, Changchun 130033, China

<sup>2</sup>University of the Chinese Academy of Sciences, Beijing 100039, China

\*yanghg@ciomp.ac.cn

**Abstract:** Generally, echelle grating ruling is performed on a thick Al film. Consequently, high-quality large-area thick Al films preparation becomes one of the most important factors to realize a high-performance large-size echelle grating. In this paper, we propose a novel multi-step deposition process to improve thick Al films quality. Compared with the traditional single-step deposition process, it is found that the multi-step deposition process can effectively suppress large-size grains growth resulting in a low surface roughness and high internal compactness of thick Al films. The differences between single- and multi-step deposition processes are discussed in detail. By using multi-step deposition process, we prepared high-quality large-area Al films with a thickness more than 10  $\mu\text{m}$  on a 520 mm  $\times$  420 mm neoceramic glass substrate.

©2015 Optical Society of America

**OCIS codes:** (310.1860) Deposition and fabrication; (240.0310) Thin films; (050.2770) Gratings; (310.3915) Metallic, opaque, and absorbing coatings.

---

## References and links

1. G. Harrison, "The Challenge of the Ruled Grating," *Phys. Today* **3**(9), 6–12 (1950).
2. J. Song, L. C. Chen, and B. J. Li, "A fast simulation method of silicon nanophotonic echelle gratings and its applications in the design of on-chip spectrometers," *Prog. Electromagnetics Res.* **141**, 369–382 (2013).
3. S. Engman and P. Lindblom, "Blaze characteristics of echelle gratings," *Appl. Opt.* **21**(23), 4356–4362 (1982).
4. P. Lindblom, "Echelle gratings acting as one," *Appl. Opt.* **42**(22), 4549–4559 (2003).
5. K. G. Bach and B. W. Bach, Jr., "Large-ruled monolithic echelle gratings," *Proc. SPIE* **4014**, 118 (2000).
6. I. S. McLean, E. E. Becklin, O. Bendiksen, G. Brims, J. Canfield, D. F. Figer, J. R. Graham, J. Hare, F. Lacayanga, J. E. Larkin, S. B. Larson, N. G. Levenson, N. Magnone, H. I. Teplitz, and W. Wong, "Design and development of NIRSPEC: a near-infrared echelle spectrograph for the Keck II telescope," *Proc. SPIE* **3354**, 566–578 (1998).
7. T. W. Barnard, M. I. Crockett, J. C. Ivaldi, and P. L. Lundberg, "Design and evaluation of an echelle grating optical system for ICP-OES," *Anal. Chem.* **65**(9), 1225–1230 (1993).
8. D. Nevejans, E. Neefs, E. Van Ransbeeck, S. Berkenbosch, R. Clairquin, L. De Vos, W. Moelans, S. Glorieux, A. Baeke, O. Korabiev, I. Vinogradov, Y. Kalinnikov, B. Bach, J. P. Dubois, and E. Villard, "Compact high-resolution spaceborne echelle grating spectrometer with acousto-optical tunable filter based order sorting for the infrared domain from 2.2 to 4.3 microm," *Appl. Opt.* **45**(21), 5191–5206 (2006).
9. G. R. Harrison, S. W. Thompson, H. Kazukonis, and J. R. Connell, "750-mm ruling engine producing large gratings and echelles," *J. Opt. Soc. Am.* **62**(6), 751–756 (1972).
10. X. T. Li, H. L. Yu, X. D. Qi, S. L. Feng, J. C. Cui, S. W. Zhang, Jirigalantu, and Y. Tang, "300 mm ruling engine producing gratings and echelles under interferometric control in China," *Appl. Opt.* **54**(7), 1819–1826 (2015).
11. Z. Z. Li, H. G. Yang, X. Y. Wang, and J. S. Gao, "Investigations of high-quality aluminum film with large-area uniformity for large-size echelle grating," *Wuli Xuebao* **63**(15), 157801 (2014).
12. J. Strong, "The evaporation process and its application to the aluminizing of large telescope mirrors," *Astrophys. J.* **83**(5), 401–423 (1936).
13. H. E. Bennett, J. M. Bennett, and J. Ashley, "Infrared Reflectance of Evaporated Aluminum Films," *J. Opt. Soc. Am.* **52**(11), 1245–1250 (1962).

14. A. P. Bradford, G. Hass, J. F. Osantowski, and A. R. Toft, "Preparation of mirror coatings for the vacuum ultraviolet in a 2-m evaporator," *Appl. Opt.* **8**(6), 1183–1189 (1969).
15. S. Wilbrandt, O. Stenzel, H. Nakamura, D. Wulff-Molder, A. Duparré, and N. Kaiser, "Protected and enhanced aluminum mirrors for the VUV," *Appl. Opt.* **53**(4), A125–A130 (2014).
16. M. Yang, A. Gatto, and N. Kaiser, "Highly reflecting aluminum-protected optical coatings for the vacuum-ultraviolet spectral range," *Appl. Opt.* **45**(1), 178–183 (2006).
17. M. Schürmann, P. J. Jobst, S. Yulin, T. Feigl, H. Heiße, S. Wilbrandt, O. Stenzel, A. Gebhardt, S. Risse, and N. Kaiser, "Optical reflector coatings for astronomical applications from EUV to IR," *Proc. SPIE* **8450**, 84502K (2012).
18. H. G. Yang, Z. Z. Li, X. Y. Wang, Z. F. Shen, J. S. Gao, and S. W. Zhang, "Radial-quality uniformity investigations of large-area thick Al films," *Opt. Eng.* **54**(4), 045106 (2015).
19. H. A. Macleod, *Thin-film optical filters*, (Taylor & Francis, 2010), Chap.13.
20. F. Villa, A. Martínez, and L. E. Regalado, "Correction masks for thickness uniformity in large-area thin films," *Appl. Opt.* **39**(10), 1602–1610 (2000).
21. J. I. Larraquert, J. A. Méndez, and J. A. Aznárez, "Life prolongation of far ultraviolet reflecting aluminum coatings by periodic recoating of the oxidized surface," *Opt. Commun.* **135**(1-3), 60–64 (1997).
22. Z. Lai and S. D. Sarma, "Kinetic growth with surface relaxation: continuum versus atomistic models," *Phys. Rev. Lett.* **66**(18), 2348–2351 (1991).
23. K. N. Tu, A. M. Gusak, and I. Sobchenko, "Linear rate of grain growth in thin films during deposition," *Phys. Rev. B* **67**(24), 245408 (2003).
24. D. J. Paritosh, D. J. Srolovitz, C. C. Battaile, X. Li, and J. E. Butler, "Simulation of faceted film growth in two-dimensions: microstructure, morphology and texture," *Acta Mater.* **47**(7), 2269–2281 (1999).
25. J. I. Larraquert, J. A. Méndez, and J. A. Aznárez, "Empirical relations among scattering, roughness parameters, and thickness of aluminum films," *Appl. Opt.* **32**(31), 6341–6346 (1993).
26. K. Robbie, J. C. Sit, and M. J. Brett, "Advanced techniques for glancing angle deposition," *J. Vac. Sci. Technol. B* **16**(3), 1115–1122 (1998).
27. T. Karabacak, "Thin-film growth dynamics with shadowing and re-emission effects," *J. Nanophotonics* **5**(1), 052501 (2011).
28. J. F. Chang, H. H. Kuo, I. C. Leu, and M. H. Hon, "The effects of thickness and operation temperature on ZnO:Al thin film CO gas sensor," *Sens. Actuators B Chem.* **84**(2-3), 258–264 (2002).
29. T. Onishi, E. Iwamura, and K. Takagi, "Morphology of sputter deposited Al alloy films," *Thin Solid Films* **340**(1-2), 306–316 (1999).
30. S. J. Hwang, J. H. Lee, C. O. Jeong, and Y. C. Joo, "Effect of film thickness and annealing temperature on hillock distributions in pure Al films," *Scr. Mater.* **56**(1), 17–20 (2007).

## 1. Introduction

Since echelle grating was invented by Harrison in 1949 [1], it has been applied extensively in spectral detection and analysis fields due to its high diffraction order, broad spectrum range, high dispersion, and excellent resolution [2–4]. Large-size echelle grating, as an extension to conventional echelle grating, can achieve a super-high spectrum resolution up to  $10^6$  owing to its extremely high diffraction order and large aperture [5,6]. Currently, it has become an essential component of various optical devices applied in astronomical observation, element detection, and high power lasers [7,8]. When the size of the echelle grating is larger than 300 mm × 300 mm, it can only be currently prepared by a grating ruling engine [9,10]. Its fabrication method is extruding and polishing Al films on a grating substrate using a diamond graver, which makes Al films generate previously designed deformations and exhibit periodic nanostructure. Consequently, Al films with excellent structural and optical properties, such as thickness uniformity, internal compactness, surface roughness, film hardness, and surface reflection, act as a critical role in echelle grating fabrication [11].

For ensuring the plasticity and shaping ability of Al films during the long-time ruling process, fabricators mostly use thermal evaporation and electron beam evaporation to prepare Al films for ordinary gratings. Although the history of Al thermal evaporation technology can be traced more than a century [12,13], the investigations of large-area Al films mainly concentrate on Al reflector coatings, which are widely utilized on a multitude of optical systems [14]. In addition, the fabrication technique of large-size Al mirror coating mostly used in the telescope is quite well-rounded and its thickness is generally fixed at a few hundred nanometers [15–17]. However, when the designed ruling depth of an echelle grating is around 5  $\mu\text{m}$ , the thickness of Al film should be 2–2.5 times of the ruling depth, 10–15  $\mu\text{m}$ , according to grating ruling experience. Unlike a conventional Al reflector, an Al film

thickness increase in echelle gratings induces lots of new problems and challenges. First of all, along with the increased thickness, continuous accumulating error enhances the difficulty of monitoring the uniformity and quality of Al films, which directly influences the diffraction wavefront quality and diffraction efficiency. Moreover, it is requisite to reduce the internal defect of Al films as much as possible for a favorable grating shape. The Al film softening leads to low diffraction efficiency and excess stray light. The most important thing for echelle grating is to have atomically flat Al surfaces. However, for almost all of the deposition techniques, the surface morphology generates a growth front roughness that causes diffraction efficiency degradation. The roughness of Al film rapidly rises with increasing thickness. Therefore, unexpectedly large surface roughness is also a fatal problem for thick Al films.

Up to now, systematic studies on properties and deposition technique of thick Al films have been rarely done, especially in echelle grating. Therefore, in this paper, we propose a novel multi-step deposition method for high-quality and large-area thick Al films. First, we present the influence of the key parameters, such as deposition structure and fixture height, on the uniformity and quality of Al films by theoretical simulation and experimental measurement. Then we demonstrate the influence of the thickness and substrate temperature on the surface roughness of Al films. Afterwards, we compare the thick Al films deposited by the traditional single- and multi-step deposition process. In addition, we analyze the improvement of surface roughness of Al films fabricated by the multi-step deposition process. In the end, we successfully prepared high-quality Al films with the thickness of more than 10 $\mu$ m, and the uniformity error less than  $\pm 1\%$  within the diameter of 800mm.

## 2. Experiment procedure

In this study, a 520 mm (length)  $\times$  420 mm (width)  $\times$  200 mm (thickness) neoceramic glass was used as the substrate material. It has an extremely low expansion coefficient, lower than conventional glass materials. Thick Al films were deposited in an electron-beam evaporation coating system with a chamber diameter of 1800 mm, which was equipped with two electron guns (TeleMark II). Figure 1 shows the schematic structure diagram of the deposition system. After chemical cleaning in acetone and ethanol, the substrate was loaded on a rotated plane fixture instead of a planetary fixture, because large-area thickness uniformity was more conveniently obtained by adjusting fixture height. In order to ensure the radial-quality uniformity of Al films, the double electron-beam co-evaporation process reported in our previous work [16] was performed to deposit thick Al films at a pressure of  $2 \times 10^{-4}$  Pa. The deposition rate was controlled at 100  $\text{\AA}/\text{s}$ , which was monitored by a quartz crystal.

Here we utilized two coating process techniques. One is the single-step deposition process. In other words, Al materials are continuously evaporated and deposited onto the neoceramic glass substrate. Another is the multi-step deposition process. In this case, thick Al films were discontinuously deposited via four steps without leaving high vacuum. The time interval is 2 hours between each step, and all the parameters such as deposition rate and film thickness are the same for all steps. Finally, we evaluated the inner structure, surface reflectance, surface roughness and hardness of thick Al films by means of a scanning electron microscope (SEM, JSM-6510 of JEOL), spectrophotometer (Lambda 1100 of PerkinElmer), atomic force microscope (AFM, EDG of Bruker) and nano indentation (Nano Indenter G200 of Agilent), respectively.

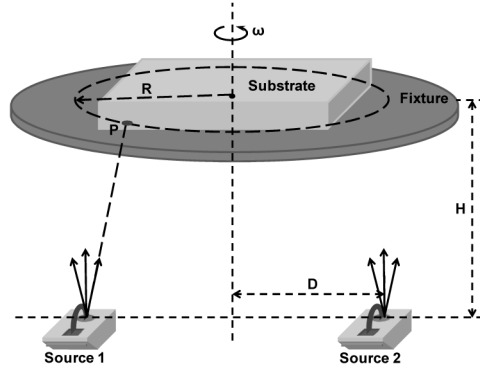


Fig. 1. A schematic structure diagram of the electron-beam evaporation coating system.

### 3. Results

Figure 2(a) shows the experimental thickness uniformity of 12  $\mu\text{m}$ -thick Al films as a function of fixture height (H) along the radial direction. It shows that the thickness uniformity is strongly dependent on H. According to film coating theory, the film thickness distribution on a rotated plane substrate can be expressed [18,19]:

$$T_p = \int_0^r C \frac{H^{(N+1)}}{\left[ H^2 + (D + R_p)^2 - 4DR_p \sin^2(\omega t / 2) \right]^{(N+3)/2}} d(\omega t) \quad (1)$$

where  $T_p$  represents the thickness at any point (P) along radius direction, C is a constant, D is the distance between system center and evaporation source as shown in Fig. 1,  $R_p$  is the radius at P,  $\omega$  is the fixture rotating speed, and N describes the evaporating characteristic of electron-beam source and keeps a constant 100  $\text{\AA}/\text{s}$  deposition rate of. According to Eq. (1), the film thickness distribution mainly depends on H. The theoretical results are also given in Fig. 1(a), which shows a good agreement with the experiment. At  $H = 1050 \text{ mm}$ , we achieved the optimal film uniformity error less than  $\pm 1\%$  within  $R = 400 \text{ mm}$ . This means that the thickness uniformity of 12  $\mu\text{m}$ -thick Al films on the  $520 \text{ mm} \times 420 \text{ mm}$  substrate can be improved to less than  $\pm 1\%$  by adjusting H in this study.

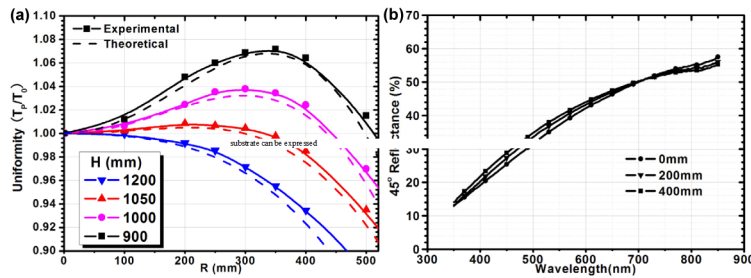


Fig. 2. (a) Both the experimental and theoretical thickness uniformity of thick Al films as a function of fixture height along the radius direction; (b) The surface reflectance of thick Al films in the visible region at various radial positions.

Besides the thickness uniformity, the uniformity of Al film quality, such as surface roughness and internal compactness, along the radius direction is also one of the most factors for grating ruling because it directly affects the groove shape and ruling efficiency [20]. Figure 2(b) shows the surface reflectance of thick Al films in the visible region at various radial positions, which the radial-quality uniformity can be confirmed because the surface reflectance is determined by surface roughness and internal compactness. Figure 2(b) shows

the surface reflectance in the whole visible region has less change along the radial direction indicating high radial-quality uniformity.

Figures 3(a) and 3(b) show the top surface AFM image and cross-sectional SEM image of 12  $\mu\text{m}$ -thick Al films created by the single-step deposition process, respectively. From Fig. 3(a), it is found that the measured surface roughness ( $R_q$ ) is as high as 64.2 nm, which seriously affects the grating efficiency because too much incident light will be lost via light scattering. In addition, it is clear from the cross-sectional image in Fig. 3(b) that some hole defects are observed in Al films, which imply that the internal structure is not dense enough by single-step deposition process. In the bottom of the Al layer in Fig. 3(b), it looks like a sharp change from compact to porous. This is because the bottom surface is unintentionally rolled up due to its high ductility.

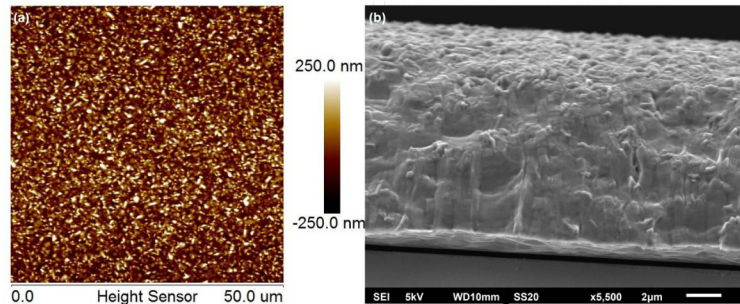


Fig. 3. (a) Top surface AFM image and (b) cross-sectional SEM images of 12  $\mu\text{m}$ -thick Al films fabricated by the single-step deposition process.

In order to improve the quality of thick Al films, we developed an alternative method, e.g. multi-step deposition process. In this case, thick Al films were discontinuously deposited by introducing four times intervals to deposition process without breaking vacuum. The time interval is 2 hours between each step. Figures 4(a) and 4(b) show the top surface AFM image and cross-sectional SEM image of 12  $\mu\text{m}$ -thick Al film created by the multi-step deposition process. By comparison with that shown in Fig. 3,  $R_q$  is reduced significantly to 24.2 nm by the multi-step deposition process, which is far lower than the 64.2 nm by the single-step deposition process. Second, for the thick Al films internal structure in Fig. 4(b) fabricated by the multi-step deposition process, it becomes much denser than the films created by the single-step deposition process. Moreover, we found that a black area existed between two Al layers. This area belongs to the upper surface of prior-deposited Al layer. During the interval time, it is possible to generate an Al oxide layer. In the work of Larruquert et al. in 1997 [21], it was reported that periodic Al oxide layers were generated between Al layers by limited exposures to atomic oxygen, leading to an increasing reflectance. However, in this study, we analyzed the interface components between Al layers by an energy dispersive x-ray (EDX) analysis, and the results showed that no obvious Al oxide layer existed. Although thick Al films exhibit a separated-layer behavior due to the interval deposition, we proved that it had no effect on the grating ruling.

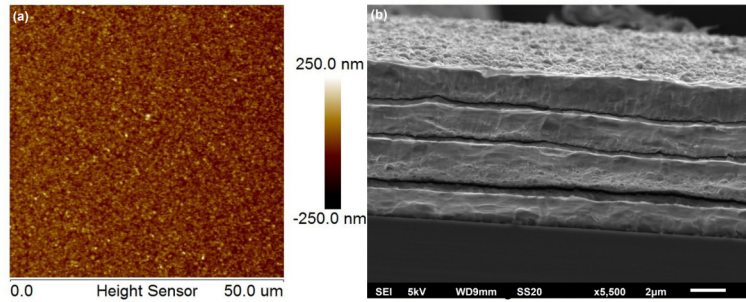


Fig. 4. (a) Top surface AFM image and (b) cross-sectional SEM images of 12  $\mu\text{m}$ -thick Al films fabricated by the multi-step deposition process.

#### 4. Discussion

In order to explain why the multi-step deposition process can improve Al film quality significantly, the thick Al film quality degradation by the single-step deposition process should be clarified. Figure 5 shows the surface AFM images of Al films with various thicknesses fabricated by the same single-step deposition process. It clearly exhibits the nano-structured nature and how the mount-like surface changes with its thickness. From the three-dimensional AFM images in Fig. 5, it can be observed that the films deposited for various film thicknesses show a uniform individual columnar grains grain size distribution extending upwards. When the thickness is thinner (1  $\mu\text{m}$ ), the surface is quite smooth and its  $R_q$  is as low as 16.3 nm, which is obtained from the AFM image directly. However, with an increased film thickness, a large amount of grains are formed on the surface and the grain grows larger. As a result,  $R_q$  gradually increased to 29.5 nm, 39.8 nm and 62.5 nm for the 4  $\mu\text{m}$ , 8  $\mu\text{m}$  and 12  $\mu\text{m}$  thick Al films, respectively.

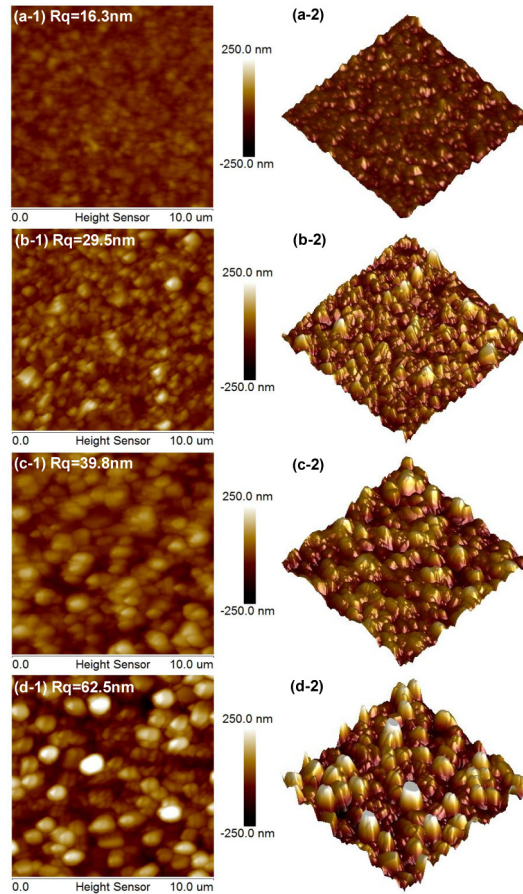


Fig. 5. Surface AFM images of Al films with various thickness fabricated by the same single-step deposition process (a) 1  $\mu\text{m}$ ; (b) 4  $\mu\text{m}$ ; (c) 8  $\mu\text{m}$ ; (d) 12  $\mu\text{m}$ .

It is known that thin film kinetic growth is a random deposition process for evaporated material [22]. According to the Van der Drift model [23,24], the random orientation nuclei are developed at the initial stage of deposition. Then the nanocrystallized structures proceed into the next competitive growth stage. Finally, crystals with a higher vertical growth rate have a greater probability for survival accompanied with growth process that causes smaller grains to aggregate and form larger grains. As a result, larger and larger grains shown in Figs. 5(a)-5(d) re formed with the increased thickness, leading to a rougher surface. Figure 6 shows both the average grain size and Rq as a function of Al film thickness, which were directly obtained from AFM images. They exhibited a similar dependence on Al film thickness and increased linearly with an increased Al film thickness. Therefore, it is concluded that Al film surface roughness is inherently due to the faceted nature of the surface mainly dependent on the grain size [25].



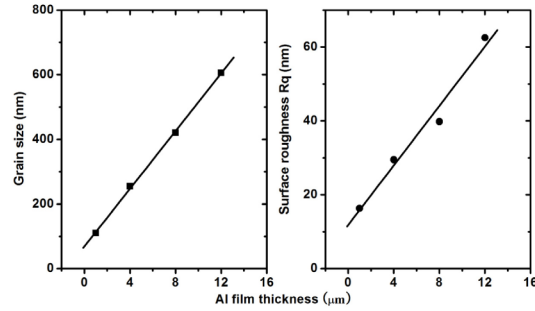


Fig. 6. The dependence of average grain size and surface roughness Rq on the thickness of Al films.

Another main factor of surface roughening should be attributed to the temperature change during the deposition process. In this study, high deposition rate of 100 Å/s is used because we found that the Al film quality became worse at a lower deposition rate. Consequently, long time deposition led to an increased substrate temperature due to tremendous thermal energy heating from deposited atoms. To clarify the substrate temperature influence on film quality, we deposited Al films at different temperatures through thermal baking. Figure 7 shows the surface AFM images of 3.5 μm-thick Al films fabricated at 100 Å/s. The corresponding baking temperatures were 100 °C, 200 °C and 300 °C, respectively. The average grain size was extracted from the AFM images. It drastically became large from 183.2 nm at 100 °C to 385.3 nm at 200 °C and 681.5 nm at 300 °C, as shown in Fig. 8. Consequently the Rq increased from 24.4 nm to 36.9 nm and 54.1 nm. These results provide powerful evidence that high deposition temperature contributes to the large size grain growth resulting in increased surface roughness.

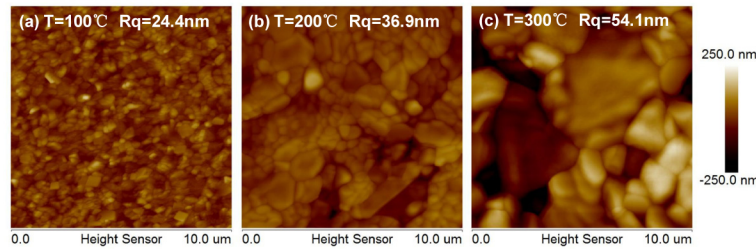


Fig. 7. AFM images of Al films deposited at various baking temperatures.

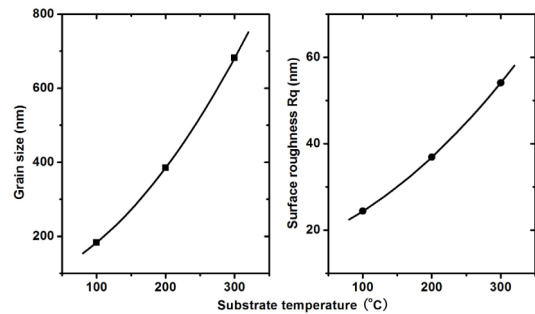


Fig. 8. The dependence of average grain size and surface roughness Rq on the substrate temperature.

The dependence of surface roughness on deposition temperature should originate from the processes affecting the morphology during Al film deposition, which involve shadowing,



surface diffusion, bulk diffusion, and sublimation energy, as reported by some groups [26–30]. Shadowing and surface diffusion can be quantified in terms of the characteristic coating surface roughness. For Al film deposition, these two mechanisms are related strongly to deposition temperature. The shadowing and surface diffusion become more dominant and consequently roughen the Al film surface at a high temperature.

Based on the analysis mentioned above, we can explain why multi-step deposition process can improve Al film quality significantly. Figure 9 shows the change profiles of substrate temperature during both single- and multi-step deposition processes, which were measured by a mechanical spring thermometer settled on the substrate. During single-step process, the substrate temperature continuously and drastically increased to a high temperature close to 200 °C. By contrast, it only stayed around 100 °C due to the cooling in the time interval of 2 hours during the multi-step process. As a result, multi-step deposition process effectively suppressed the growth of large-size grains and consequently significantly improved the quality of thick Al films. In addition, each step during multi-step deposition process is a re-growth of Al films, which means that the continuous growth of grains will be possibly interrupted resulting in decreased grain size and surface roughness. By the multi-step deposition process, as shown in Fig. 10, we successfully achieved large-area thick Al films with low surface roughness and high interval compactness on neoceramic glass substrate. Its high quality will contribute to an efficient echelle grating improvement and provide a favorable technique support for the subsequent echelle grating ruling studies.

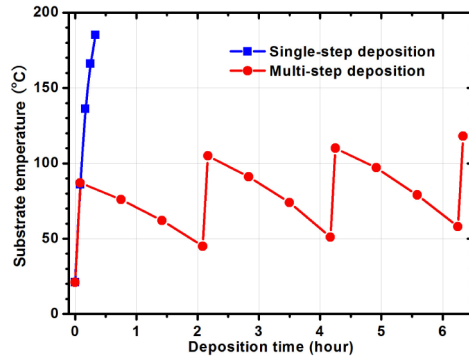


Fig. 9. Change profiles of substrate temperature during both single- and multi-step deposition processes.

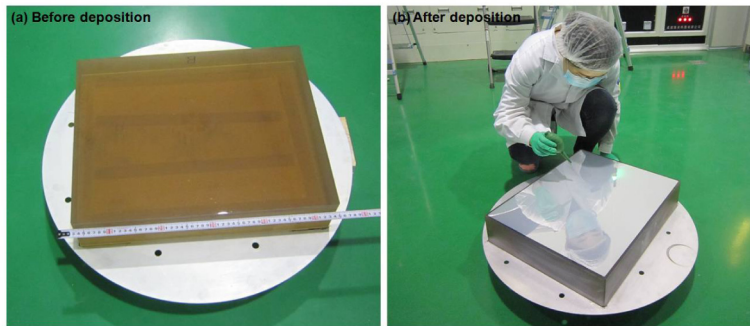


Fig. 10. (a). Neoceramic glass substrate with size of 520 mm × 420 mm × 200 mm; (b). Large-area thick aluminum films deposited on neoceramic glass substrate.

## 5. Conclusion

In summary, we investigated the preparation of large-area thick Al films by both single- and multi-step deposition processes. In the case of single-step deposition process, thick Al films

exhibit high surface roughness and low internal compactness, which were attributed to long time continuously growth of Al film and a drastic increase in deposition temperature resulting in a large amount of large-size grains. In contrast, the multi-step deposition process effectively suppressed the growth of large-size grains by controlling the deposition temperature via cooling in the time interval. As a result, we successfully prepared large-area thick Al films with low surface roughness and high internal compactness on a 520 mm × 420 mm neoceramic glass substrate. Its high quality will contribute to an efficiency improvement of echelle gratings.

### **Acknowledgments**

This research is supported by the National Key Scientific and Research Equipment Development Foundation of China (No. ZBY2008-1), the Ministry of National Science and Technology for National Key Basic Research Program of China (No. 2014CB049500), the National Natural Science Foundation of China (No. 61306125 and U1435210), the Science and Technology Innovation Project (Y3CX1SS143) of CIOMP, the Science and Technology Innovation Project of Jilin Province (No. Y3293UM130, 20130522147JH, and 20140101176JC).